Citation

M.-S. Kim, A. C. Assafrao, T. Scharf, C. Rockstuhl, S. F. Pereira, H. P. Urbach, H. P. Herzig, "Longitudinal-differential phase distribution near the focus of a high numerical aperture lens: Study of wavefront spacing and Gouy phase," J. Mod. Opt. **60**(3), 197-201 (2013).

Longitudinal-differential phase distribution near the focus of a high numerical aperture lens: Study of wavefront spacing and Gouy phase

Myun-Sik Kim[a]*, Alberto da Costa Assafrao[b], Toralf Scharf[a], Carsten Rockstuhl[c], Silvania F. Pereira[b], H. Paul Urbach[b] and Hans Peter Herzig[a]

[a]*Optics & Photonics Technology Laboratory, Ecole Polytechnique Fédérale de Lausanne (EPFL) Breguet 2, 2000 Neuchâtel, Switzerland;* [b]*Optics Research Group, Delft University of Technology, Lorentzweg 1, 2628 CJ Delft, The Netherlands;* [c]*Institute of Condensed Matter Theory and Solid State Optics, Abbe Center of Photonics, Friedrich-Schiller-Universität Jena, 07743 Jena, Germany*

*Corresponding author. Email: myunsik.kim@epfl.ch and kim@suss.com

We present a longitudinal-differential (LD) phase distribution near the focus of a high numerical aperture (NA=0.9) aplanatic lens illuminated with a linearly polarized monochromatic plane wave. The Richards and Wolf method is used to compute field distributions. The LD phase map is obtained by analyzing the deviation of the phase of the simulated wave to the phase of a referential plane wave. We discuss the irregular wavefront spacing that is linked to the Guoy phase and disclose subtle details of the phase features with respect to the spatial domain relative to the focal point. The LD phase is used to revisit different definitions of the focal region. We eventually identify the definition that is in agreement with the Gouy phase in the focal region. Our work paves the way towards a coherent notion to quantify the optical action of high NA optical elements that are increasingly important for many applications.

Keywords: Gouy phase anomaly; longitudinal-differential phase; axial phase shift; singular optics; physical optics.

1. Introduction

Structured light in focal regions is of significant interest; not only for fundamental optical problems but also in advanced optical systems. In high-resolution optical systems, for example, a tight focus is used to mediate the interaction of light with nano-sized specimens. It is known that the axial phase shift, i.e., the Gouy phase, plays an important role in the optical response of optical systems when focusing light [1-3]. Therefore, numerous studies were devoted to understand light in focal regions, the phase distributions in general, and the Gouy phase in specific. The first general picture of the phase distribution near the focus has been given by Linfoot and Wolf in 1956 [4]. There, scalar diffraction theory has been used.

Among various phase features of focused light, the wavefront shape and its spacing are mainly related to the Gouy phase. The wavefront spacing of a focused wave is known to be different to that of a plane wave of same frequency [3-12]. For low NA lenses describable by scalar diffraction theory, the wavefront spacing is increased when compared to a plane wave by the factor of

$$\alpha = \frac{1}{1 - a^2 / 4f^2} = \frac{1}{1 - \left(\frac{\mathrm{NA}}{2} \right)^2}, \qquad (1)$$

with *a* being the radius of the lens aperture and *f* being the focal length [4]. It suggests that the wavefront spacing gets larger for an increasing NA. For the non-paraxial case, i.e., when the system has a high numerical aperture, the vectorial character of light can no longer be neglected and a scalar description becomes inaccurate. Therefore, vector diffraction theory is in general necessary to provide accurate information on the subtle details of the phase features near the focus, especially on the wavefront spacing near the high NA focus [6-8]. For the high NA case, Dubois *et al.* [6] derived the increment factor β,

$$\beta = 1 + 0.25\mathrm{NA}^2 + 0.1\mathrm{NA}^4 + 0.086\mathrm{NA}^6, \qquad (2)$$

which is accurate only for the $\pm 1^{st}$ wavefront spacing away from the focal plane [8] and loses its applicability for positions a few wavelengths away from the focus. In Foley and Wolf's work [8], the vector diffraction theory by Richards and Wolf [13] has been used to simulate the wavefront spacing. They also found that the wavefront spacing near the focus is significantly increased, i.e., for the $\pm 1^{st}$ wavefront spacing away from the focal plane. The results can be predicted by the analytical solution in Equation (2) and an increment of 31% for an NA=0.9 system has been found. Moreover, the wavefront spacing drastically changes within a few wavelengths around the focus and can be even smaller than the wavelength. Various studies report on such wavefront spacing of high NA system, e.g., for linearly polarized incidence [6, 8], for three Cartesian components of the electric field [9], for radial polarization [10, 11], for partially coherent light [12], and for astigmatic focus [14]. However, the 2D or 3D full field distributions are rarely presented, measured, or discussed (for the examples see Refs. 3, 4, and 9).

In this study we present field distributions and the longitudinal-differential (LD) phase distribution near the focus of an NA=0.9 aplanatic lens. We demonstrate the irregular wavefront spacing of the high NA focus and discuss the phase properties linked to the Gouy phase anomaly. We concentrate not just on the fundamental π shift but also on subtle modulations outside the focal region. The LD phase distribution is an excellent means to discuss all these aspects since it corresponds to the difference in phase advance of the field with respect to a plane wave. With these insights we revisit various definitions for the focal region of high NA systems.

2. Simulation of the longitudinal-differential phase distribution

We employ the Richards and Wolf method [13] that solves the diffraction integral to simulate the field distributions near the focus of an NA=0.9 aplanatic lens in air. We assumed as illumination a linearly polarized (along the *x*-axis) plane wave at a wavelength of 642 nm. The computational domain is 5 x 5 x 10 μm^3 in the *xyz*-space. Figure 1(*a*) shows the intensity distribution in the *x-z* plane, which is the normalized energy density of the total electric field, i.e.,$|E_t|^2 = |E_x|^2 + |E_y|^2 + |E_z|^2$. Here, E_x, E_y, and E_z are the complex electric field components. For the axial phase study, since on the optical axis only the E_x component has a non-vanishing amplitude, the phase of E_x is used to derive the absolute and the LD phase distributions. They

are shown in Figures 1(*b*) and 1(*c*), respectively. By definition, the Gouy phase of a focused, monochromatic field at an axial point is defined as the difference between the phase of the object field and that of a plane wave of the same frequency [12]. Therefore, the LD phase map of Figure 1(*c*) is obtained by subtracting the phase of an on-axis plane wave from the calculated phase shown in Figure 1(*b*). First of all, the comparison between the intensity and the phase maps is impressive. Far away from the focal spot, which is located around $z = -1$ to 1 μm, there is practically no amplitude noticeable. In contrast, the phase demonstrates impressively the evolution of the wavefronts also outside the focal spot. The LD phase distribution clearly shows the evolution of the phase anomalies of each Airy ring; including the main Airy disc. This confirms the predictions that the off-axis Gouy phase occurs more gradual than the on-axis Gouy phase [4, 12, 14].

3. Investigation of Gouy phase

When studying the Gouy phase, the most interesting region of interest (ROI) is usually on-axis. Even though the full 3D field maps allow to analyze not only the on-axis but also the off-axis, we concentrate therefore in the following on the on-axis data. The on-axis profiles of the intensity and phase distributions extracted from Figure 1 are shown in Figure 2. For reference, the phase of a plane wave is also plotted. The absolute phase profile shows the wavefront spacing of the focused field near the focus. Before and behind the focal plane ($z = 0$ μm), the wavefront spacing is approximately $\lambda/4$ larger than that of the plane wave. It leads to the overall axial phase shift of $\lambda/2$ ($= \pi$) in the LD phase profile. This is also shown as the half-period shift between the phase of the plane wave and the absolute phase behind the focus ($z = 0$ to 5 μm), corresponding to a π phase shift behind the focal plane $z > 0$ μm. Recently, Tyc [15] showed the same consequence by analytically comparing the amplitudes of the $\mathrm{sinc}(kx)$ and $-\sin(kx)$ functions with k = wave number and x = propagation distance, which does not predict the irregular wavefront spacing away from the focal region.

As reported by Foley and Wolf [8], the wavefront spacing near the high NA focus is quite irregular. Outside the focal region ($z = -5$ to -1 μm or 1 to 5 μm), the irregular wavefront spacing produces a wavy modulation in the LD phase profile. It is shown in more detail in Figure 3. By the convention applied here [12], the positive (negative) slope of the LD phase indicates that the wavefront spacing is smaller (larger) than λ, corresponding to **Region I** (**II**) in Figure 3. Positive and negative slopes periodically repeat until the Gouy phase affects the phase evolution around the focal region ($z = -1$ to 1 μm). This modulation phenomenon can already be witnessed in Figure 1(*c*) as small spots along the axial direction ($x = 0$ μm). Due to the small variation of the wavefront spacing and the periodicity in the slope, the modulation of the phase shift remains bounded within $\pm 0.3\pi$. For the field distribution in this spatial domain, the scalar theory by Linfoot and Wolf [4] predicts phase discontinuities instead of this continuous wavy modulation. In the scalar theory they occur where the amplitude is zero. The associated phase singularities would be characterized by a π phase jump. In contrast, the vector field as investigated here does not show such singularities, clearly identifying them as artifacts inherent to the scalar approximation.

The most important and interesting region is just before and behind the focal plane around $z = 0$ μm. There, the wavefront spacing is approximately 25% (before) and 32 % (behind) larger than that of the plane wave (i.e., the wavelength λ). These results are in good agreement with predictions from the analytical solution given in Equation (2). The drastic increase of the local effective wavelength for converging and diverging fields sums up to approximately $\lambda/2$ that corresponds to a π shift in the LD phase profile (see the red solid curve in Figure 2).

4. Definition of the focal region with respect to the Gouy phase

To make use of the precise understanding of the wavefront spacing, we incorporate its variation to define the spatial extent of the focal region for high NA beams and revisit multiple definitions that were already put forward for this purpose. The definition of the focal region for the high NA focus is not a trivial task when compared to Gaussian beam theory for the low NA focus, in which the paraxial approximation and scalar theory are applicable [16]. We consider three definitions for the focal region and compare them to a criterion which exploits the wavefront spacing. To be precise, we understand as the focal region the spatial domain across which the Gouy phase is accumulated, that is a π phase difference with respect to the plane wave. The three definitions for the focal regions are the depth of focus (DOF) using the axial Rayleigh criterion [17], the axial full width at half maximum (FWHM) size, and the Rayleigh range Z_R of the Gaussian beam [16]. Those established definitions are related to the peak intensity and the spot sizes. Figure 4 shows the intensity and the LD phase profiles in the focal region at $z = -2$ to 2 μm and indicates the axial phase shift values for each definition of the focal region.

First, for the DOF, the Rayleigh criterion is applied to the axial direction as the peak intensity falls down to 80% [17]. Scalar wave theory leads to the full width of the DOF as a Rayleigh unit, $R_u = \lambda/(n \cdot \sin^2\theta)$ with n being the refractive index of the focal space and θ the focal angle. By using the NA, the Rayleigh unit can be rewritten as $R_u = n \cdot \lambda/NA^2$. This leads to 792 nm, which shows a discrepancy with the simulation result of 600 nm seen in Figure 4. The reason of the discrepancy could be the difference between the scalar and the vector approaches. The axial phase shift within the DOF shifts by 0.46π. Second, the position of the FWHM of the longitudinal profile is straightforwardly shown in Figure 4, which is at $z = \pm 0.52$ μm. Here, the axial phase shift equals 0.77π. Third, the classical Rayleigh range (Z_R) is the distance where the transverse spot size increases by a factor of √2. The z position for the transverse spot size increased by √2 is found at $z = \pm 0.73$ μm in Figure 1(*a*). In Gaussian beam theory, the Gouy phase within the Rayleigh range ($\pm Z_R$) is quantified to be 0.5π. However, for our case, the Gouy phase within $\pm Z_R$ equals 1.1π. It simply demonstrates that the vector nature of light prevents applying scalar theory and approximated Gaussian beam theory to the problems of the highly focused light. Considering the 0.5π phase shift as the set-point, the DOF using the axial Rayleigh criterion seems the most adequate definition of the focal region for the higher NA systems. For instance, the simulations for different NAs, e.g., NA = 0.5 and 0.7, lead to the same consequence. Since the analytical solution for the Rayleigh unit by scalar theory is not accurate enough, the rigorous simulation is necessary to define the DOF in that case.

5. Conclusion

We have demonstrated the longitudinal-differential phase distribution near the focus of an NA=0.9 aplanatic lens. The on-axis wavefront spacing just before and behind the focus is approximately a quarter wavelength enlarged and the sum leads to λ/2 that represents the Gouy phase shift of π. Using this phase shift as the criterion to define the depth of focus, it was found that when compared to the approximated and scalar theories, the DOF defined by the Rayleigh criterion properly indicates the focal region of the higher NA systems. The irregular wavefront spacing outside this focal region where the π shift (i.e., the Gouy phase) occurs, is repeatedly larger and smaller than λ. Such an irregularity produces the wavy modulation in the LD phase profile, which normally appears in scalar theory as discontinuous modulations. Even though the field distributions near the focus have been intensively

investigated, our approach to demonstrate the LD phase distribution out of the absolute phase map has a significant importance because it directly visualize the axial phase shift along the longitudinal plane for both on- and off-axes ROIs.

Acknowledgements

The research leading to these results has received funding from the European Community's Seventh Framework Programme FP7-ICT-2007-2 under grant agreement n° 224226.

References

[1] Gouy, L. G. *C. R. Acad. Sci.* **1890**, *110*, 1251–1253.
[2] Gouy, L. G. *Ann. Chim. Phys.***1891**, *24*, 145–213.
[3] Born, M.; Wolf, E. *Principles of Optics* (7th ed.); Cambridge University Press: Cambridge, UK, 1999.
[4] Linfoot, E. H.; Wolf, E. *Proc. Phys. Soc. B* **1956**, *69*, 823–832.
[5] Li, Y.; Wolf, E.; Gbur, G.; Visser, T. D. *J. Mod. Opt.* **2004**, *51*, 779–781.
[6] Dubois, A.; Selb, J.; Vabre, L.; Boccara, A. *Appl. Opt.* **2000**, *39*, 2326–2331.
[7] Chang, F. C.; Kino, G. S. *Appl. Opt.* **1998**, *37*, 3471–3479.
[8] Foley, J. T.; Wolf, E. *Opt. Lett.* **2005**, *30*, 1312–1314.
[9] Pang, X.; Visser, T. D.; Wolf, E. *Opt. Commun.* **2011**, *284*, 5517–5522.
[10] Visser, T. D.; Foley, J. T. *J. Opt. Soc. Am. A* **2005**, *22*, 2527–2531.
[11] Chen, H.; Zhan, Q.; Zhang, Y.; Li, Y.-P. *Phys. Lett. A* **2007**, *371*, 259–261.
[12] Pang, X.; Fischer, D. G.; Visser, T. D. *J. Opt. Soc. Am. A* **2012**, *29*, 989–993.
[13] Richards, B; Wolf, E. *Proc. R. Soc. London Ser. A* **1959**, *253*, 358–379.
[14] Visser, T. D.; Wolf, E. *Opt. Commun.* **2010**, *283*, 3371–3375.
[15] Tyc, T. *Opt. Lett.* **2012**, *37*, 924–926.
[16] Siegman, A. E. *Lasers*; Univerty Science books: Palo Alto, USA, 1986; Chap. 17.
[17] Gross, H.; Zugge, H.; Peschka, M.; Blechinger, F. *Handbook of Optical Systems* (Vol. 3); Wiley-VCH: Darmstadt, Germany, 2007; pp 126.

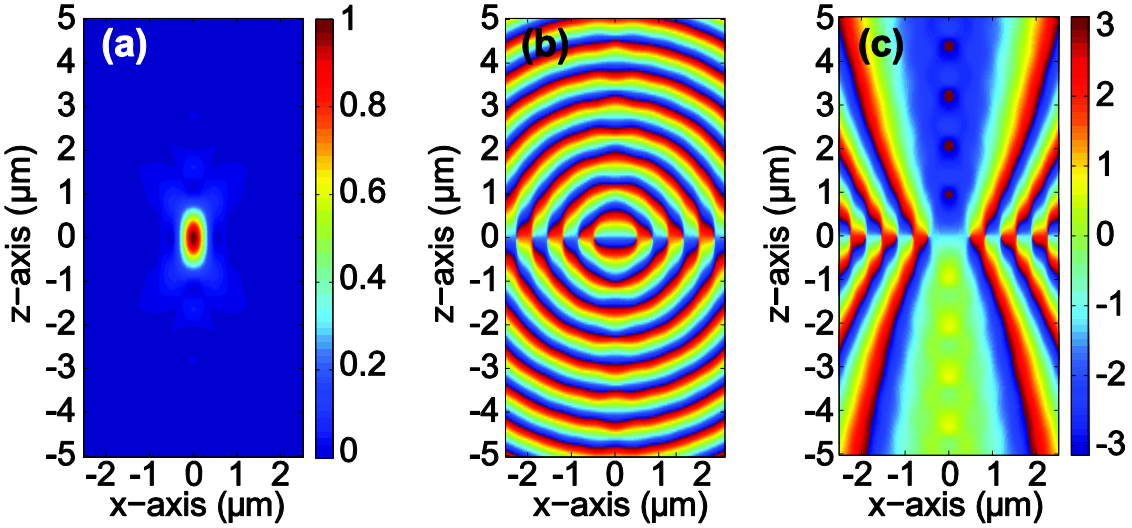

Figure 1. Simulated field distributions near the focus in the x-z plane: (a) intensity, (b) absolute phase, and (c) longitudinal-differential phase maps. The intensity is normalized and the phase is in radian from $-\pi$ to π. The aplanatic focal plane is at z = 0 μm. (The color version of this figure is included in the online version of the journal.)

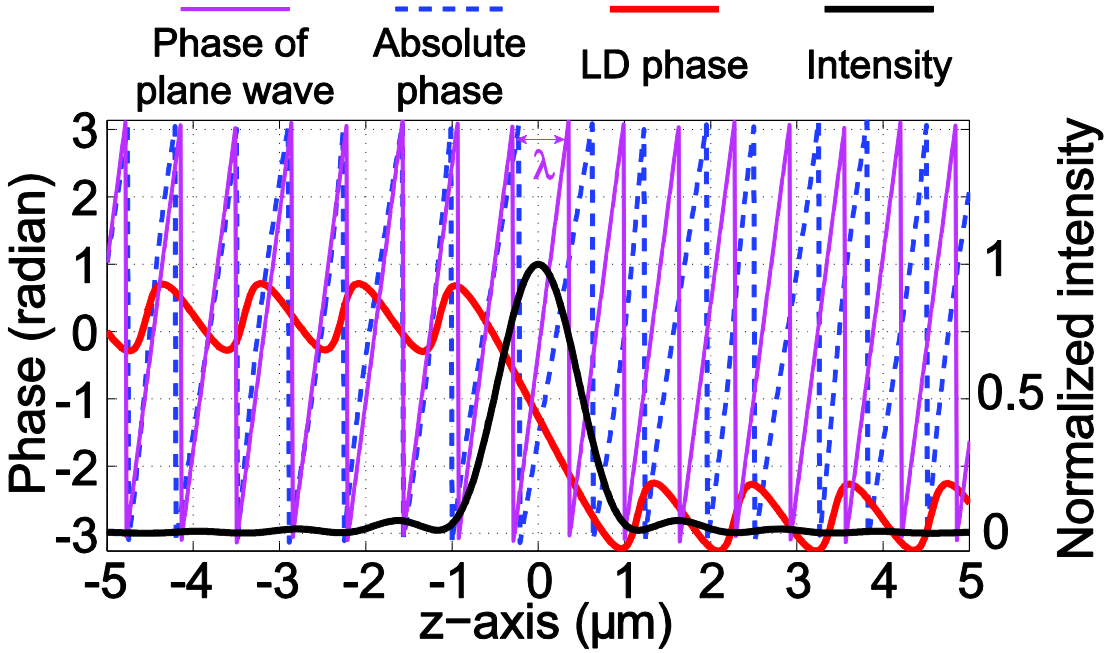

Figure 2. On-axis phase and intensity profiles extracted from Figure 1. (The color version of this figure is included in the online version of the journal.)

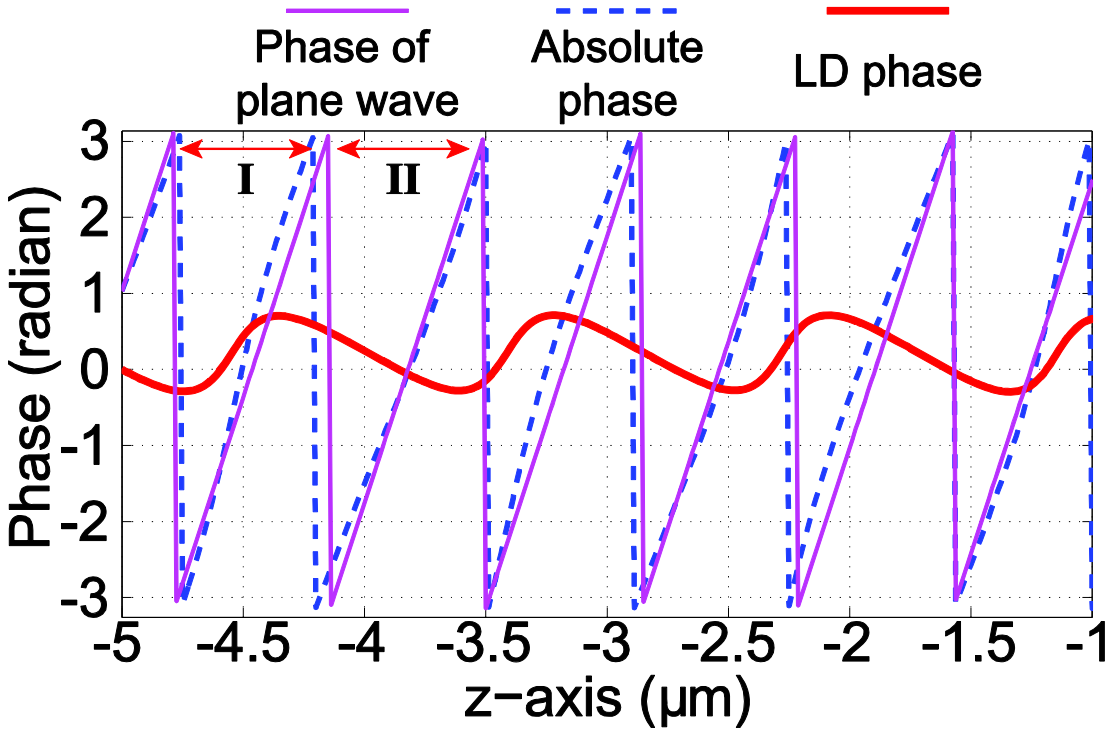

Figure 3. The phase profiles outside the focal region before the focus (z = –5 to –1 μm). (The color version of this figure is included in the online version of the journal.)

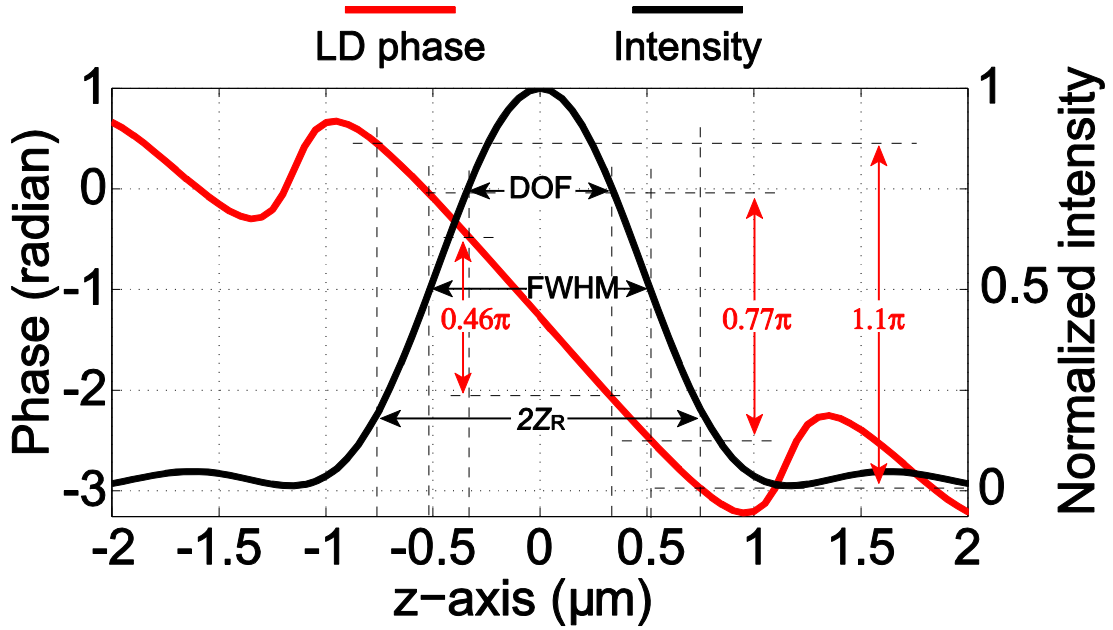

Figure 4. The LD phase and intensity profiles in the focal region (z = –2 to 2 μm) with indications on various criteria investigated in this work. (The color version of this figure